Sensors & Actuators: B. Chemical 300 (2019) 126907

Contents lists available at ScienceDirect

Sensors and Actuators B: Chemical

journal homepage: www.elsevier.com/locate/snb

# Optofluidic label-free SERS platform for rapid bacteria detection in serum

Robert Hunter[a,*], Ali Najafi Sohi[b], Zohra Khatoon[c], Vincent R. Berthiaume[d], Emilio I. Alarcon[c,e], Michel Godin[a,b,f], Hanan Anis[g]

[a] Ottawa-Carleton Institute for Biomedical Engineering, University of Ottawa, Ottawa, Ontario, K1N 6N5, Canada
[b] Department of Physics, University of Ottawa, Ottawa, Ontario, K1N 6N5, Canada
[c] Cardiac Surgery Research, University of Ottawa Heart Institute, Ottawa, Ontario, K1Y 4W7, Canada
[d] Department of Chemical and Biological Engineering, University of Ottawa, Ottawa, Ontario, K1N 6N5, Canada
[e] Department of Biochemistry, Microbiology, and Immunology, Faculty of Medicine, University of Ottawa, Ottawa, Ontario, K1N 6N5, Canada
[f] Department of Mechanical Engineering, University of Ottawa, Ottawa, Ontario, K1N 6N5, Canada
[g] School of Electrical Engineering and Computer Science, University of Ottawa, Ottawa, Ontario, K1N 6N5, Canada

ARTICLE INFO

*Keywords:*
Surface enhanced Raman scattering
Optofluidic
Label-free detection
Machine learning
Hospital acquired infection

ABSTRACT

The prevalence of hospital acquired infections and antibiotic resistant pathogens necessitates the development of bacteria sensing systems that do not require sample amplification via conventional cell culturing, which can be prohibitively time-consuming. To meet this need, we designed an optofluidic Raman detection platform which utilized a microfluidic driven hollow-core photonic crystal fiber, which in combination with silver nanoparticles, provides a large enhancement to the Raman signal. By confining both light and cells within this fiber, spectral events generated by the flowing cells facilitates a novel method of cell counting to simultaneously quantify and qualify infections. Counting is performed automatically by a genetically optimized support vector machine learning algorithm that was previously developed by our group. The microfluidic system can be regenerated multiple times, and allows for online detection of planktonic bacteria to levels as low as 4 CFU/mL in 15 min. This compares favourably to other methods currently under development such as qPCR and biosensing techniques. Furthermore, Raman spectral differences between bacteria allow for inherent multiplexed detection in serum, by adding another layer to the learning algorithm. Further development of this device has promising potential as a rapid point-of-care system for infection management in the clinic.

## 1. Introduction

Healthcare associated infections (HAI), also known as nosocomial infections, are recognised as a global public health issue [1]. The incidence of HAI ranges from 17 infections per 1000 patient-days in high income countries, to over 40 in middle to low income countries [1]. This translates to around 6 million episodes of HAI in Europe and North America every year. These infections are frequently caused by medical devices, such as catheters, permanent implants, or ventilators, which are inserted into patients during a variety of procedures. The use of such devices may introduce components of the patient's own microbiome into their bodies and cause infection [2]. Furthermore, due to the increased use of antibiotics, the presence of antimicrobial resistant pathogens may further complicate the infection [3]. Early diagnosis and screening of antimicrobial resistant pathogens is important for making informed treatment decisions [4]. However, standard microbial culture analysis requires several hours, or even days to produce a reliable answer on the pathogen identity. Thus there is a present need to develop more rapid analytical methods.

Some new technological approaches to bacterial screening, including qPCR and biosensors, are increasingly gaining attention as faster and more precise alternative tools. Rather than detecting the bacteria itself, qPCR based techniques indirectly quantify the microbe by using their nucleic acid, necessitating additional components such as primers, probes, and DNA extraction solutions [5]. Others have reported the use of biosensing techniques such as surface plasmon resonance (SPR) [6–9], and electrical impedance spectroscopy (EIS) [10–12]. Raman spectroscopy is another promising technique which measures the inelastic scattering of light from molecular vibrational modes in a sample [13]. This signal is rather weak, so surface enhanced Raman spectroscopy (SERS) leverages the strong electric field in the vicinity of metal nanostructures to enhance this scattering. The resulting spectrum is a unique molecular fingerprint of the sample being assayed, which can be used to detect, quantify, and discriminate

* Corresponding author.
*E-mail address:* rhunt009@uottawa.ca (R. Hunter).

https://doi.org/10.1016/j.snb.2019.126907
Received 8 May 2019; Received in revised form 12 July 2019; Accepted 30 July 2019
Available online 31 July 2019

biochemically distinct samples. SERS is frequently employed in the analysis of liquids, thus this technique lends itself well to the development of integrated optofluidic platforms, of which many have been developed for various applications [14]. An important consideration when designing an optofluidic SERS system for bacterial analysis is whether to use a label-free approach, or to apply bio-recognition elements such as antibodies or aptamers [15]. Label-free techniques facilitate inherent multiplexing due to intrinsic differences in SERS spectra from bacteria, however it becomes difficult to decompose the spectrum if multiple bacteria are present. Conversely, labeled approaches allow for greater control of specificity, but limit the system to bacteria that can be captured by the SERS substrate. Previously reported SERS devices for bacteria detection using capture elements include bimetallic nanoparticles with aptamers and Raman reporter molecules for multiplexed bacteria detection [16], and aptamer coated gold and magnetic nanoparticles for *S. aureus* and *S. typhimurium* detection [17]. Examples of the label free approach include a microfluidic system which mixes bacteria and silver nanoparticles for SERS detection [18], and SERS with vancomycin coated silver-gold nanoparticles for detection of bacteria in blood [19]. In some applications it may be necessary to concentrate the bacteria before SERS measurement. This has been shown in the microfluidic dielectrophoresis enrichment system developed by Wang et al to obtain SERS spectra of bacteria at dilute concentrations [20].

Previously, our group has developed a system for acquiring Raman spectra from a hollow-core photonic crystal fiber (HC-PCF) [21]. When the fiber is filled with fluid, it is capable of simultaneously coupling light and samples within a small space. This effectively increases the depth of focus of the laser to the length of HC-PCF, thereby significantly increasing the fluid/field overlap and amplifying the Raman signal generated within. Yang et al. have previously utilized a HC-PCF enhanced SERS system to detect bacteria by capillary filling of the fiber and subsequent acquisition of spectra [22]. However, we have previously found that filling by capillary action decreases the robustness of a fiber enhanced Raman system because the filling can be inconsistent, and one then needs to throw away an expensive fiber after the measurement is complete [23]. Furthermore, relying on Raman spectra of bulk fluid is not applicable in cases where the bacterial density is low. This is because there is a chance that the fiber is filled with fluid containing few or no bacteria, which severely hinders the limit of detection. It may be better therefore to count the cells as they actively flow through the fiber in a method similar to flow cytometry, and then restoring the fiber with a cleaning solution. Fluorescence based flow cytometry is an indispensable tool in cellular analysis, and Raman spectra can be used in place of the fluorescent markers. For example, dye and antibody conjugated nanoparticles have been used to detect cancer cells in a SERS flow cytometer [24], and a microfluidic trap built over plasmonic nano-dimers could acquire Raman spectra of single cells flowing in blood plasma [25]. Counting of bacteria using antibody and aptamer labelled SERS has been explored recently with promising results [26]. In this work, we seek to combine single cell counting of bacterial SERS with the enhancement afforded by HC-PCF coupled spectroscopy. Additionally, we employ simple nanoparticles and rely on a powerful new machine learning algorithm to differentiate between types of bacteria in a label-free system, which will increase the potential breadth of applicability when compared to labelled methods. This results in a system that is capable of detecting 4 CFU/mL within only minutes. This technology will be a breakthrough in the clinic by allowing direct identification of bacterial infections in the operating room, even at levels ordinarily undetectable, helping to considerably improve the clinical outcome of hundreds of thousands of patients globally.

## 2. Materials

Ethanol, silver nitrate salt, sodium citrate tribasic dihydrate, lysogeny broth (LB) medium, agarose, and rhodamine 6G (R6G) were all purchased from Sigma-Aldrich. Fetal bovine serum (FBS) was acquired from Gibco. The three bacteria species studied in this work *Pseudomonas aeruginosa* (PA01), *Staphylococcus aureus* (ATCC 25923), and *Escherichia coli* (CFT073) were acquired from ATCC and cultured following the recommended guidelines. The polydimethyl-siloxane (PDMS) with curing agent was Sylgard 184 purchased from Dow Corning. Hollow core photonic crystal fiber used in this work was HC-1550 from Thorlabs.

## 3. Methods

### 3.1. Synthesis and analysis of silver nanoparticles

Silver nanoparticles were prepared using the citrate reduction method. Briefly, 50 mL of a 1.2 mM solution of silver nitrate in deionized water was brought to a boil while stirring at 700 rpm. Once a boil was obtained, 10 mL of 1% w/v sodium citrate was added. This solution was subsequently boiled for 1 h, followed by submersion into ice water in order to stop the reaction. The result was a yellow-grey silver colloid composed of approximately $3.3 \times 10^9$ particles/mL with a mean diameter of ~100 nm. This solution was stored away from ambient light at 4 °C. Under these conditions, the silver nanoparticles were found to be stable for a period of several months. The nanoparticles were analysed by means of transmission electron microscopy (TEM) imaging and UV–vis absorption spectroscopy.

### 3.2. Fabrication of optofluidic device

The microfluidic device was 24 × 14 × 3.5 mm in size and made of PDMS using replica molding. The master mold consisted of microchannel features made from SU8 photoresist spin coated over a 4-inch silicon wafer. The microchannel was 12.6 mm in length and had a $100 \times 60$ μm$^2$ (width, height) rectangular cross section. The PDMS used to produce the microchannel was mixed at base/curing agent ratio of 10:1 (w/w) followed by degassing in a vacuum for 45 min. and curing at 70 °C for 2 h. Two 0.75 mm holes were punched at the ends of the microchannel for interfacing with polytetrafluoroethylene (PTFE) tubing. Additionally, a 1.25 mm hole was punched in the middle of the microchannel for interfacing with the optical fiber via a sleeve. Following hole punching, the PDMS was permanently bonded to a 75 × 25 × 1.0 mm microscope glass slide (VWR VistaVision) using air plasma at 50 W for 30 s. For completion of the bond, the device was left at 70 °C overnight.

Following the fabrication of the microfluidic devices, the channels were integrated with the HC-PCF to form the final optofluidic device. All components were filled with ethanol during assembly in order to guarantee that there were no bubbles present in the system. A piece of HC-PCF was used to bridge the two microfluidic channels and affixed with epoxy resin. Finally, the device is flushed with deionized water and is ready to be integrated into the optical system.

### 3.3. Acquisition of fiber enhanced Raman spectra

The system used to acquire Raman spectra consists of a 785 nm wavelength laser, whose power was controlled by a current/temperature regulator. This laser light is collimated by a gradient index (GRIN) lens, reflected by an adjustable mirror through a bandpass filter centred at 785 nm, and then reflected by a dichroic mirror into a 0.65 numerical aperture (NA) plano-convex aspheric lens which is used to couple the light into the optofluidic device. This device is mounted on a Thorlabs compact 3-axis flexure stage via a custom 3D printed chassis. Khetani et al. have shown that the bandgap of an HC-PCF blue-shifts when a material of higher refractive index is introduced into the core and cladding channels [23]. In this case, the bandgap which is normally centred at 1550 nm when filled with air (n = 1.0) is shifted to

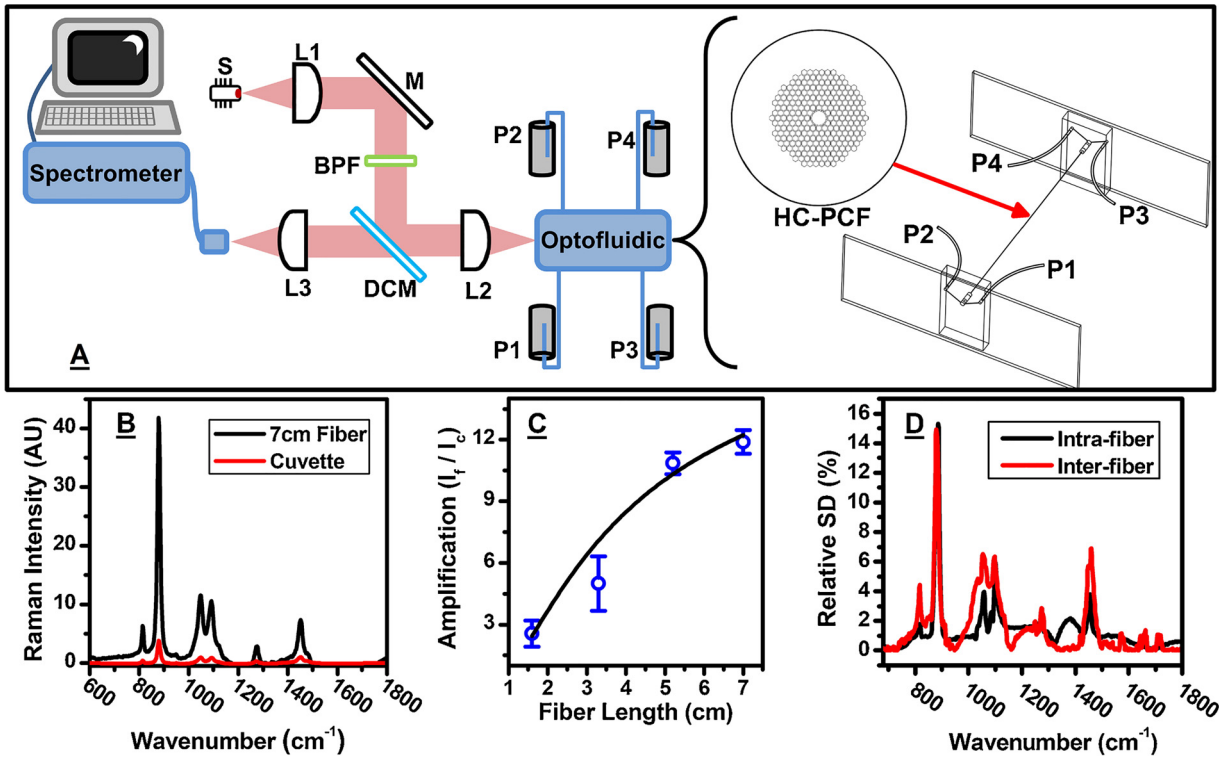


**Fig. 1.** Summary of the general performance results of the Raman optofluidic platform. (A) Drawing of the optofluidic system along with the microfluidic and HC-PCF. The 785 nm laser source is represented by S, L1 is the GRIN lens, L2 and L3 are plano-convex lenses of NA = 0.65 and 0.3 respectively, M is an adjustable mirror, BPF is the laser-line bandpass filter, DCM is a longpass dichroic mirror, P1-4 are pressure sources connected to the optofluidic platform that push fluid from reservoirs through the system as described in Section 3.3. (B) Raman spectra of ethanol in cuvette and a 7 cm piece of HC-PCF. (C) Ratio of fiber intensity to cuvette intensity as a function of fiber length, black line is an exponential best fit. (D) Relative standard deviation (SD) of the Raman spectrum measured from 12 fill/flush cycles (intra-fiber deviation), and the deviation between four different fibers (inter-fiber deviation).

approximately 785 nm when the device is filled with water (n = 1.34). The coupling into the HC-PCF was optimized by simultaneously adjusting the flexure stage and the adjustable mirror in order to obtain single-mode coupling efficiencies between 40–50%. The Raman scattered photons generated within the fiber are collected by the same aspheric lens. These Stokes shifted photons pass through the dichroic mirror and are coupled into a multimode collection fiber via a 0.3 NA plano-convex aspheric lens. This fiber leads into a Kaiser f/18i Spectrograph with a TE-cooled Andor CCD camera equipped with Andor SOLIS software. Unless otherwise noted, the current delivered to the laser was set to 70 mA resulting in ~15 mW of power, and the integration time was 1 s.

In order to fill the fiber, a 4-pressure system was used as shown in Fig. 1A, wherein each pressure source is connected to a fluid reservoir. In all experiments P1 was connected to the sample reservoir, P3 was connected to the flushing reservoir, and P2 and P4 were connected to waste reservoirs. Initially, P1 was increased to 70 kPa in order to charge the microfluidic device with the analyte of interest. Subsequently P2 was set to equal P1 in order to the halt lateral flow, and both were increased to 200 kPa to force the fluid through the HC-PCF. Finally, P3 was set to be 15 kPa in order to continuously flush the analyte away from the tip of the fiber, and P4 was left at atmospheric pressure. After measurement, all pressures were dropped to atmospheric pressure, and the fiber was then flushed. Flushing the fiber was performed identically to the aforementioned filling process except P3 and P4 were set to high pressure in order to fill the fiber in the reverse direction with the flushing fluid. The flow of the flushing fluid was maintained for 5 min. and the fluid itself was dependant on the analyte used, as will be discussed in later sections.

The samples containing bacteria in FBS were mixed in a 1:1 ratio with the previously synthesized silver colloid. This solution was allowed to incubate while the optofluidic platform was being flushed after the previous measurement, which required 5 min. This solution was pumped into the HC-PCF in accordance to the procedure outlined above. The spectrograph was set to acquire one spectrum every second for a period of 10 min. from the fiber.

### 3.4. Culture and counting of bacteria

Bacteria cultures for quantification were produced by taking 10 µL of bacteria suspension and streaking this fluid onto a LB agar plate. These plates where incubated at 37 °C for 16 h. Afterwards, a single colony was taken with an inoculation loop and suspended in 2 mL of LB medium, which was again incubated for 16 h. This procedure produced bacteria samples containing ~$10^9$ CFU/mL. This sample was then diluted in pure FBS to create the samples with low concentrations of bacteria, which were then stored at 4 °C and used within 24 h for Raman quantification. In order to quantify the samples against the conventional counting method, 5 µL of a $10^5$ CFU/mL solution of bacteria was plated onto LB agar plates and incubated at 37 °C for 16 h. The colonies on each plate were then counted in order to get an estimate for the number of CFU in each sample. Mixed samples were prepared in an identical fashion, in that each bacterium was cultured and counted separately. Subsequently, the individual preparing the samples added an amount of each bacterium to FBS, the quantity of which was known to the preparer but unknown to the operator of the optofluidic system.

### 3.5. Data analysis

Raman spectra were processed in MATLAB for all analyses. The exact methodology used was dependant on the analyte from which the spectra were obtained and the intended application of the data. In

general, the pre-processing consisted of background subtraction using the method developed by Kandjani et al, using a fifth order polynomial to fit the background [27]. If the spectra were to be used for classification analysis, they were then normalized by dividing by the highest observed intensity. Furthermore, for bacteria samples, the SERS spectrum of the background matrix was also subtracted from the signal.

The classification analysis was performed by either projection to latent structures discriminant analysis (PLS-DA) using built in MATLAB functionality, or by genetic support vector machines (GA-SVM). The GA-SVM algorithm is explained and analysed in detail in a previous report by our group [28]. In short, a classical genetic algorithm is combined with SVMs to facilitate the use of complex kernel functions when analysing high dimensional datasets. SVMs essentially compare data points on the basis of a kernel function $\kappa$, which is some metric of the similarity between two points. Using this kernel function, which describes some feature space constructed from the data, the SVM seeks an optimal separating hyperplane in said feature space. In this work, we have explored the rational quadratic kernel (RQK) as the basis for the GA-SVM models. This kernel, which approximates an infinite sum of Gaussian kernels, is shown in Eq. (1):

$$\kappa_{RQK} = \sigma^2\left(1 + \frac{(x_i - x_j)^2}{2\alpha l^2}\right)^{-\alpha} \quad (1)$$

where $\sigma$, $\alpha$, and $l$ are kernel hyperparameters that must be selected to generate a good model and $x$ is the dataset containing all of the Raman spectra wherein $i$ and $j$ represent two of said spectra [29]. These are optimized by the genetic algorithm which compares SVM models using a fitness function which rewards models that are simultaneously robust and accurate. In order to extend the SVM from the usual binary classification case to the multi-class case the “one-against-one” multi-binary classifier method was used.

When utilizing either PLS-DA or GA-SVM, models were trained using 60% of the dataset for model generation and the remaining 40% for validation. All reported results pertaining to the performance of these analysis methods are from the validation sets, which were not included in training the algorithm. The accuracy of prediction was then used to compare the different algorithms. In order to quantify the bacteria, a two-layer classifier was used. The first layer discriminates bacteria spectra from the background serum spectra. The next layer classifies the spectra into one of the three bacteria species studied in this paper. This system was used to automatically count the number of bacterial spectral events in a given time frame and then correlating this to the density of cells in the sample. The limit of detection was then calculated based on $LOD = 3\sigma_B$ wherein $\sigma_B$ is the standard deviation of the blank sample.

## 4. Results and discussion

In order to be clinically applicable, a detection system must be reproducible and accurate. We begin with optimizing the system using simple fluids and dye molecules. We show that the fiber can be filled with sample and subsequently flushed in a reproducible manner and that the HC-PCF system plus the silver nanoparticles provides a greater signal enhancement than either of these alone. Next, this system is applied to the analysis of bacteria in FBS. By balancing the pressures across the microfluidic chips, it is possible to force all of the sample flow through the HC-PCF. Therefore, any bacteria which pass through the system must pass through the laser light coupled into the fiber, and generate Raman scattering therein. Taking advantage of this, we have developed a novel method of counting the spectral events generated by the bacteria as they pass through the fiber, and correlating the number of counts to the density of bacteria in the sample. The aforementioned GA-SVM is used to automate this counting, and is compared to simpler linear methods. As an initial proof of concept, we have used clinically relevant bacteria strains, namely *S. aureus* (SA), *E. coli* (EC), and *P. aeruginosa* (PAO1) to validate the system and analyse its ability to perform multiplexed measurements.

### 4.1. Optofluidic Raman platform performance

The performance of the optofluidic system pictured in Fig. 1A was first evaluated using ethanol to understand the effect of fiber length on Raman enhancement and the fill/flush reproducibility of the system. Fig. 1B shows the Raman spectrum of pure ethanol as measured from a cuvette compared to that collected from a 7 cm piece of HC-PCF. In this case we observe an approximately twelvefold enhancement caused by the HC-PCF compared to the simple cuvette measurement. This ratio is calculated based on the peak at 880 $cm^{-1}$ where $I_c$ is its intensity in cuvette and $I_f$ is the intensity in the fiber. Fig. 1C illustrates how this enhancement changes as a function of length. For this experiment, the range of fiber length is limited to approximately 0.5 to 8 cm due to the design of the chassis that supports the microfluidic system in front of the coupling lens. As will be shown in later sections, this range was more than sufficient for the present application. The fiber gain increases in an exponential fashion as the length of the fiber increases. From the regression shown in Fig. 1C, we expect that the enhancement continues to level-off beyond lengths of 7 cm. This is likely caused by two factors. Firstly, longer fibers are more difficult to fill perfectly bubble free, therefore as the length increases the probability of bubble filled sections decreasing the coupling efficiency also increases. Secondly, the bandgap of the fiber is centred about the coupled wavelength of 785 nm. Therefore, the Raman shifted photons are carried less efficiently along the length of the fiber, and Raman photons generated at the distal end are less likely to be guided along the entire length.

Fig. 1D examines both intra- and inter-fiber reproducibility. We observe that the relative standard deviation between 12 fill/flush cycles is less than 5–15% of the peak intensity. For four different fiber pieces, we observe a relative inter-fiber deviation of approximately 7–15%. The reproducibility of the system is acceptable for the current application because the spectra are normalized before being processed by the discriminant algorithms. In cases where the absolute magnitude of the spectrum is important, it may be necessary to improve the reproducibility. This may be achieved by automating the fiber cleaving and coupling processes, as these are currently done manually. Overall, this microfluidic system is an improvement over our previous optofluidic sensor that used high performance liquid chromatography connections [23]. The enhancement and the reproducibility are comparable to the old system, but the dead fluid volume is decreased by an order of magnitude, and the microchannels are far easier to manufacture.

### 4.2. SERS performance

Next we investigated the performance of a silver colloid as a SERS substrate within the optofluidic system. Fig. 2A shows the Raman spectrum of 100 μM R6 G dye in water in three different conditions. We see that the spectrum of R6 G in the cuvette is weak and poorly resolved. The peak-baseline difference is on the order of 60 counts/s for the strongest peak at 1345 $cm^{-1}$. The addition of the silver colloid to the solution of R6 G increases this peak intensity about 200 fold. Subsequent injection of this solution through the optofluidic platform enhances the signal by an additional twofold, thus the total bulk enhancement of the optofluidic platform with SERS substrate is about 400 fold over a simple diffraction limited system. Fig. 2B shows a TEM image of the silver nanoparticles. From the TEM images we find that the colloid is composed primarily of mono and poly-disperse particles with some nanoplates and rods. In this application, lasing at 785 nm was used to excite Raman scattering due to the excellent penetrance of near infra-red wavelengths into biological media [30] The silver nanoparticles synthesized here are quite large and poly-disperse, as shown by the TEM image as well as the broad absorption spectrum in Fig. 2D. These larger structures facilitate excitation of localized plasmon

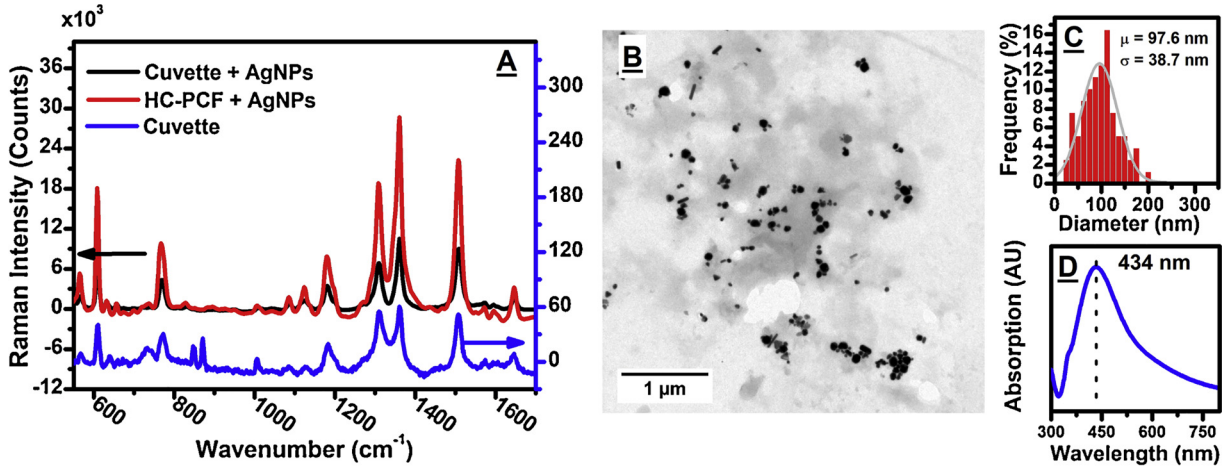


**Fig. 2.** Results of initial SERS validation for the optofluidic Raman platform. (A) Raman spectra of R6 G in cuvette (blue curve and blue y-axis), and SERS spectra of R6 G in cuvette and HC-PCF (black y-axis). (B) TEM image of the silver nanoparticles on a copper grid. (C) Size distribution of silver nanoparticles. (D) UV Vis absorption spectrum of the silver nanoparticles.

resonance modes at longer wavelengths. Interestingly we have found that the twofold fiber enhancement is relatively independent of the length of the fiber, and does not seem to increase as a function of the length. If we apply the curve shown in Fig. 1C, we see that the effective length of the fiber is only 1.5 cm. This is likely due to the absorption and scattering by these relatively large silver nanoparticles which greatly attenuate the propagation of the light along the fiber. For all future SERS experiments, HC-PCF pieces around 3 cm in length were used in order to have sufficient length to easily mount the fiber in the optofluidic system.

During the initial SERS experiments, it was found that flushing the system with deionized water alone did not regenerate the platform, thereby greatly compromising the reusability of the system. By flushing the system with methanol, into which R6 G is far more soluble than in water, we found that it was possible to fully regenerate the system between measurements. This highlighted the necessity of choosing a flushing liquid that was capable of fully removing any analyte in the HC-PCF to ensure complete system regeneration.

### 4.3. Mono-culture bacteria analysis in fetal bovine serum

After validating the reproducibility and the amplification of the optofluidic detection platform, the device was used to analyse bacteria present in FBS to simulate clinical samples. As noted earlier, three different bacteria were used for an initial validation for the system, namely PAO1, SA, and EC. Average post-processed SERS spectra for each of these bacteria are shown in Fig. 3A, as well as the average spectrum of the background, and the standard deviation of all the spectra. These averages were taken from the training sets used to generate the GA-SVM models, thus they contain spectra from the entire span of three 10-min. measurements. We observe negligible deviation of the FBS spectrum, illustrating that the spectral output from the optofluidic platform is stable between and during measurements. As bacteria cells pass through the fiber, a very strong SERS signal is generated over a short time-of-flight period as the cell passes through the strong field region in the proximal 1.5 cm of the optical fiber. It was hypothesized that the optofluidic platform could be used to count the number of spectral events over a given time frame, and that this count would correlate to the bacterial density in the sample.

In order to perform the counting automatically, it was necessary to implement a classifier which could distinguish between the background spectrum and the bacteria spectra. Furthermore, in order to create a multiplexed system a second classifier layer would need to discriminate between the types of bacteria based on their SERS spectrum. A conventional method to construct classifiers when confronted with large multivariate datasets is PLS-DA, which is a linear method related to principal component analysis and Fischer discriminants. We have compared this method to our GA-SVM algorithm, on the ability to appropriately label the genus of a bacterial spectrum.

In order to train the algorithms, sets of spectra were acquired from dense monocultures ($10^9$ CFU/mL) of each bacterium in order to generate a library of bacterial SERS spectra. Approximately 500 spectra were acquired from three separate samples for each of the three bacteria to generate the total known set. We observed that GA-SVM significantly outperforms PLS-DA in this application, achieving ˜92% accuracy compared to ˜56% for PLS-DA ($p < 10^{-8}$). Given that there are three potential classes, the accuracy for a random guess for this problem is approximately 33%. Therefore, there is evidently some information that can be obtained from a linear discriminant, but only by allowing for the non-linear solutions of the GA-SVM can a good model be obtained. The full confusion matrix showing this model's ability to distinguish bacteria spectra from the background and differentiate between species is shown in Table 1. Previous comparison between these two algorithms on their classification ability showed only a small difference between them [28]. This was very likely due to the linear separability of the test sets used in the past. In the present scenario, there is a stochastic element to the SERS spectra, likely due to the non-specific binding of the silver nanoparticles to the bacteria. This can be seen in the relative standard deviations of the bacterial spectra in Fig. 3A. The relative deviation can be on the same order of magnitude as the spectral components themselves. Particularly in the case of PAO1, some peaks may be completely absent between spectral events. This causes a large degree of within-class variance in the datasets, thus classification and regression problems will be solved much better with a highly non-linear tool like a kernelized SVM.

The GA-SVM was then used to perform automatic counting of spectral events from samples with bacterial loads ranging from 0 to 100 CFU/mL. An event was defined as a change from the background spectrum to a bacterial spectrum and back to the background. It should be noted that the theoretical time of flight for a cell passing through the fiber may be greater than one second. Assuming the cells are moving with the maximum velocity at the center of the fiber, by the Darcy-Weisbach equation the cells would be travelling at approximately 1.5 cm/s. For this reason, spectral events that occur consecutively are counted as a single event. Fig. 3B–D show the calibration models obtained for each bacterium using the number of events counted over a period of 10 min. Using this system, the limit of detection for bacteria in FBS ranges from 3.2 to 4.3 CFU/mL with good linearity ($R^2 > 0.9$). In

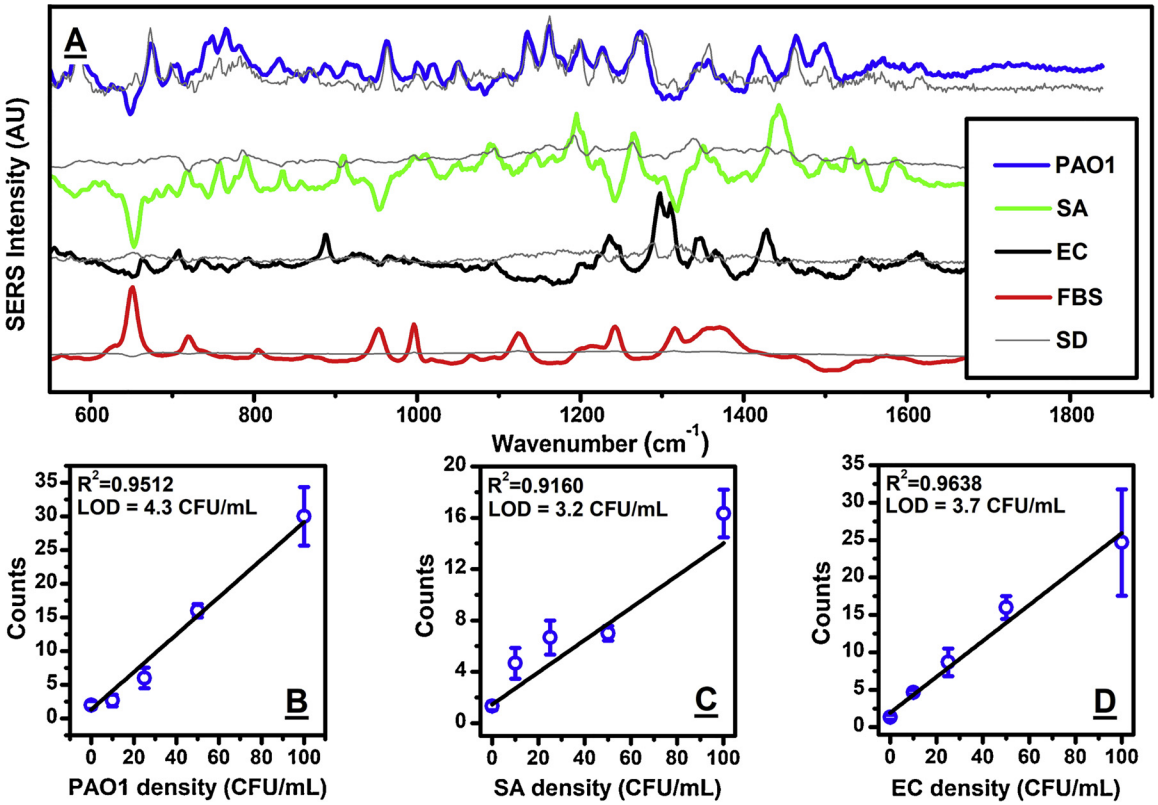


**Fig. 3.** Summary of the detection performance of the device for monocultures of bacteria in fetal bovine serum (FBS). (A) Representative SERS spectra of *P. aeruginosa* (PAO1), *S. aureus* (SA), and *E. coli* (EC), as well as FBS and the relative stnadard deviation (SD) of each spectrum. (B-D) PAO1, SA, and EC density in FBS as a function of spectral events in a 10 min. window, respectively.

**Table 1**
Confusion matrix showing the results of the dual layer SVM used to count bacterial spectral events.

| | | *Predicted* | | | |
|---|---|---|---|---|---|
| | | Matrix | PAO1 | EC | SA |
| *True* | Matrix | 93.6% | 0.0% | | |
| | PAO1 | 6.4% | 92.5% | 6.7% | 0.8% |
| | EC | | 4.0% | 90.5% | 5.5% |
| | SA | | 1.0% | 1.4% | 97.6% |

**Table 2**
The measured vs. actual bacteria density in five blind samples.

| Blind Sample | PAO1 (CFU/mL) actual / measured | SA (CFU/mL) actual / measured | EC (CFU/mL) actual / measured |
|---|---|---|---|
| A | 10 / 16.64 | 10 / 7.77 | 10 / 13.68 |
| B | 0 / -2.57 | 25 / 19.59 | 50 / 43.23 |
| C | 0 / -7.00 | 0 / -1.09 | 0 / 4.82 |
| D | 25 / 4.82 | 25 / 29.94 | 25 / 35.85 |
| E | 25 / 15.16 | 100 / 103.81 | 50 / 91.99 |

order to regenerate the system between measurements, the system was flushed with a 1.0% solution of Triton x100 followed by deionized water.

### 4.4. Mixed culture bacteria analysis in fetal bovine serum

Having constructed the spectral databases, the calibration models, and the associated GA-SVM classifiers, the performance of the opto-fluidic SERS platform as a multiplexed system was analysed. To this end, blind samples were generated whose bacterial type and density were unknown to the operator of the detector. In this analysis, we assume that each measured spectral event belongs to only one bacterial set. This must be the case, because the GA-SVM models are built based on samples containing a single type of bacteria. If the GA-SVM fails to properly discriminate spectra in mixed samples, then this would indicate that the spectra of bacterial mixtures are substantially different from those shown in Fig. 3A. The results from this experiment are summarized in Table 2. We observe an imperfect, but well correlated ($R^2$ = 0.96) match between the standard culture-based analysis and the SERS detector. Overall, the strong correlation indicates that using spectra from monoculture samples can be applied to the analysis of mixed samples. The overall root mean squared error is 13.27 CFU/mL, which is most pronounced in blind samples D and E where the load of PAO1 is underestimated, and the load of EC is overestimated. This would suggest that some PAO1 events are being misclassified as EC events. Indeed, we observe in the confusion matrix shown in Table 1 that this was the most commonly observed misclassification. Additionally, the SA concentrations are well estimated by the system, which is in further agreement with the confusion matrix. As of now, there is no inherent viability metric employed by this system, the true CFU/mL is not actually measured but rather an effective CFU/mL. Therefore, dead cells and cell fragments likely contribute to the count of each bacteria type. In many cases it is likely that cell fragments of different bacteria may have similar SERS spectra, hence the erroneous classification that appears to be observed in samples with higher bacterial loads. It is well known that nano-silver has a bactericidal effect, therefore this may increase the number of dead cells in the sample. It has been shown that the minimum inhibitory concentration of citrate capped silver nanoparticles for EC is approximately 50 μM of total silver. In approximately 1 h, these particles reduce the number of viable cells by one order of magnitude from a $10^5$ CFU/mL starting culture [31]. In this experiment about 60 μM of total silver is used, thus cell

**Table 3**
Comparison of different novel methods for bacteria sensing including surface plasmon resonance (SPR), electrical impedance spectroscopy (EIS), surface enhanced Raman scattering (SERS), and quantitative polymerase chain reaction (qPCR) assays.

| Transducing Element | Limit of Detection (CFU/mL) | Time Required | Ref. |
|---|---|---|---|
| HC-PCF enhanced SERS counting | 3.2–4.3 | 15 min. | This work |
| SPR with gold nanohole array | 100 | 35 min. | [6] |
| SPR with gold film, anti-fouling layer, and gold nanoparticle sandwich | 17–7400 | 80 min. | [7] |
| SPR with aptamer on gold coated silica nanoparticles | 10,000 | 60 min. | [8] |
| EIS on gold electrode with antibody | 10 | Not specified | [10] |
| EIS on interdigitated gold electrodes with antibody-gold nanoparticles | 100 | 5 min. | [11] |
| EIS on lectin functionalized gold electrode | 75 | 60 min. | [12] |
| SERS with dielectrophoresis enrichment and functionalized gold nanorods | 1 | 17 hrs | [20] |
| SERS with aptamer conjugated silver nanoparticles | 15 | 20 min. | [26] |
| Duplex droplet digital PCR | 4000 | 70 min. | [34] |
| qPCR | 10 | 120 min. | [35] |

death due to the particles is likely. However, the incubation time is very short at 5 min, with an additional 10 for the measurement. In previous work by our group, it was found that differences between states of death in leukaemia cells could be distinguished using Raman spectroscopy [32]. Therefore, an additional classifier could potentially be applied using live/dead data in order to get a true CFU measurement, which may improve results.

### 4.5. Comparison to other methods

A number of technologies are currently being explored to replace standard culture methods. The time requirement and performance of culture based analyses vary between different approaches and applications. For example, according to clinical practice guidelines for the diagnosis of prosthetic joint infection, it is recommended to acquire at least three samples for aerobic/anaerobic culture during surgery [33]. These samples may be incubated for up to 14 days in order to detect pathogens, and this is followed by histopathological analysis. This method achieves sensitivity and specificity on the order of 80% and 90% respectively, and theoretically even a single CFU can be isolated after incubation. When possible, it is recommended that antimicrobial treatment be withheld until this process is finished, since the appropriate treatment is dependent on the infecting pathogen. In order to apply treatment as soon as possible, it is imperative that new technologies accelerate this process, ideally by removing the need to culture samples.

Table 3 shows the detection limit and time requirements of different methods reported in the literature. All of these new methods significantly reduce the time requirement when compared to culturing, but the detection limit varies significantly among these technologies. Given that isolating one CFU can be considered a positive sample in some applications, it is evident that improvements to these new technologies are still necessary. The fiber enhanced SERS counting method examined in this work compares favourably to PCR, SPR, EIS, and other SERS methods. Furthermore, this work utilizes silver nanoparticles without any surface functionalization. The GA-SVM algorithm facilitates inherent multiplexing by virtue of the differences between bacterial SERS spectra. Multiplexing in other techniques requires additional primers, or other bio-recognition elements.

## 5. Conclusion

In summary, we have designed an optofluidic Raman platform which utilized a hollow-core photonic crystal fiber filled via microfluidics as the main transducing element. This system can be regenerated repeatedly, by flushing the system with a fluid into which the analyte of interest is soluble. Addition of silver nanoparticles into the system provides a large bulk enhancement to the Raman scattered field which facilitates measuring the spectra of biological molecules which tend to have low Raman cross-sections. This system has been applied to the multiplexed detection of bacteria in FBS, wherein a novel method of forcing bacteria to flow through the hollow fiber and counting the number of Raman events was developed. This counting was preformed automatically using a powerful genetic SVM algorithm. This system achieved a detection limit on the order of 4 CFU/mL while requiring only minutes to perform a measurement. In Canada, this device would be considered a relatively high risk diagnosis device (Class III) because it is used to inform treatment decisions for potentially antibiotic resistant transmissible pathogens. Therefore, more development is necessary before this this system can be used in clinics. This development must include investigational clinical testing, comparing the results to both culturing methods and qPCR, and improving the system performance. The current LOD is acceptable for some forms of HAI, but others require a still lower limit. For example, in severe bacteraemia cases, the circulating levels of bacteria can be as low as 1 CFU/mL [36]. Additionally, for applications in space-limited situations such as in a surgical theater, the footprint of the system should be reduced, possibly by the use of integrated optics. Following approval, this platform represents an exciting path to a rapid point-of-care system, which will be valuable to clinicians in a number of disciplines.

## CRediT authorship contribution statement

**Robert Hunter:** Conceptualization, Methodology, Software, Validation, Formal analysis, Investigation, Writing - original draft, Visualization. **Ali Najafi Sohi:** Methodology, Resources, Writing - review & editing. **Zohra Khatoon:** Investigation, Resources. **Vincent R. Berthiaume:** Validation, Investigation. **Emilio I. Alarcon:** Writing - review & editing, Supervision, Project administration. **Michel Godin:** Writing - review & editing, Supervision. **Hanan Anis:** Writing - review & editing, Supervision, Project administration, Funding acquisition.

## Declaration of Competing Interest

The authors do not possess any potential conflicts of interest regarding this work.

## Acknowledgements

This research in Dr. Anis' lab was supported by the Natural Sciences and Engineering Research Council of Canada (NSERC) Discovery Grant #210374-181099-2001. Work in Dr. Godin's lab was supported by The Canada Foundation for Innovation (CFI). Work in Dr. Alarcon's lab was supported by NSERC RGPIN-2015-0632 and the Canadian Institutes of Health Sciences (CIHR).

## References


[1] World Health Organization, Report on the Burden of Endemic Health Care-Associated Infection Worldwide, (2011).

[2] A. Kropec, J. Huebner, M. Riffel, U. Bayer, A. Benzing, K. Geiger, E.D. Daschner, Exogenous or endogenous reservoirs of nosocomial Pseudomonas aeruginosa and Staphylococcus aureus infections in a surgical intensive care unit, Intensive Care Med. 19 (1993) 161–165, https://doi.org/10.1007/BF01720533.

[3] A.W. Friedrich, Control of hospital acquired infections and antimicrobial resistance in Europe: the way to go, Wiener Med. Wochenschr. 169 (2019) 25–30, https://doi.org/10.1007/s10354-018-0676-5.

[4] C.F. Lowe, K. Katz, A.J. Mcgeer, M.P. Muller, Toronto ESBL working group, efficacy of admission screening for extended-spectrum beta-lactamase producing enterobacteriaceae, PLoS One 8 (2013) 1–8, https://doi.org/10.1371/journal.pone.0062678.

[5] M.G. Quiles, L.C. Menezes, K. de C. Bauab, E.K. Gumpl, T.T. Rocchetti, F.S. Palomo, F. Carlesse, A.C.C. Pignatari, Diagnosis of bacteremia in pediatric oncologic patients by in-house real-time PCR, BMC Infect. Dis. 15 (2015) 1–8, https://doi.org/10.1186/s12879-015-1033-6.

[6] J. Gomez-Cruz, S. Nair, A. Manjarrez-Hernandez, S. Gavilanes-Parra, G. Ascanio, C. Escobedo, Cost-effective flow-through nanohole array-based biosensing platform for the label-free detection of uropathogenic E. coli in real time, Biosens. Bioelectron. 106 (2018) 105–110, https://doi.org/10.1016/j.bios.2018.01.055.

[7] H. Vaisocherová-Lísalová, I. Víšová, M.L. Ermini, T. Špringer, X.C. Song, J. Mrázek, J. Lamačová, N. Scott Lynn, P. Šedivák, J. Homola, Low-fouling surface plasmon resonance biosensor for multi-step detection of foodborne bacterial pathogens in complex food samples, Biosens. Bioelectron. 80 (2016) 84–90, https://doi.org/10.1016/j.bios.2016.01.040.

[8] S.M. Yoo, D.K. Kim, S.Y. Lee, Aptamer-functionalized localized surface plasmon resonance sensor for the multiplexed detection of different bacterial species, Talanta 132 (2015) 112–127, https://doi.org/10.1016/j.talanta.2014.09.003.

[9] I. Yazgan, N.M. Noah, O. Toure, S. Zhang, O.A. Sadik, Biosensor for selective detection of E. coli in spinach using the strong affinity of derivatized mannose with fimbrial lectin, Biosens. Bioelectron. 61 (2014) 266–273, https://doi.org/10.1016/j.bios.2014.05.008.

[10] K. Bekir, H. Barhoumi, M. Braiek, A. Chrouda, N. Zine, N. Abid, A. Maaref, A. Bakhrouf, H. Ben Ouada, N. Jaffrezic-Renault, H. Ben Mansour, Electrochemical impedance immunosensor for rapid detection of stressed pathogenic Staphylococcus aureus bacteria, Environ. Sci. Pollut. Res. 22 (2015) 15796–15803, https://doi.org/10.1007/s11356-015-4761-7.

[11] N. Pal, S. Sharma, S. Gupta, Sensitive and rapid detection of pathogenic bacteria in small volumes using impedance spectroscopy technique, Biosens. Bioelectron. 77 (2016) 270–276, https://doi.org/10.1016/j.bios.2015.09.037.

[12] H. Yang, H. Zhou, H. Hao, Q. Gong, K. Nie, Detection of Escherichia coli with a label-free impedimetric biosensor based on lectin functionalized mixed self-assembled monolayer, Sens. Actuators B Chem. 229 (2016) 297–304, https://doi.org/10.1016/j.snb.2015.08.034.

[13] P.J. Larkin, IR and Raman Spectroscopy: Principals and Spectral Interpretation, Elsevier Inc., 2011.

[14] C. Lim, J. Hong, B.G. Chung, A.J. DeMello, J. Choo, Optofluidic platforms based on surface-enhanced Raman scattering, Analyst 135 (2010) 837–844, https://doi.org/10.1039/b919584j.

[15] Y. Liu, H. Zhou, Z. Hu, G. Yu, D. Yang, J. Zhao, Label and label-free based surface-enhanced Raman scattering for pathogen bacteria detection: a review, Biosens. Bioelectron. 94 (2017) 131–140, https://doi.org/10.1016/j.bios.2017.02.032.

[16] S.P. Ravindranath, Y. Wang, J. Irudayaraj, SERS driven cross-platform based multiplex pathogen detection, Sens. Actuators B Chem. 152 (2011) 183–190, https://doi.org/10.1016/j.snb.2010.12.005.

[17] H. Zhang, X. Ma, Y. Liu, N. Duan, S. Wu, Z. Wang, B. Xu, Gold nanoparticles enhanced SERS aptasensor for the simultaneous detection of Salmonella typhimurium and Staphylococcus aureus, Biosens. Bioelectron. 74 (2015) 872–877, https://doi.org/10.1016/j.bios.2015.07.033.

[18] N.A. Mungroo, G. Oliveira, S. Neethirajan, SERS based point-of-care detection of food-borne pathogens, Microchim. Acta. 183 (2015) 697–707, https://doi.org/10.1007/s00604-015-1698-y.

[19] A. Sivanesan, E. Witkowska, W. Adamkiewicz, Ł. Dziewit, A. Kamińska, J. Waluk, Nanostructured silver-gold bimetallic SERS substrates for selective identification of bacteria in human blood, Analyst 139 (2014) 1037–1043, https://doi.org/10.1039/c3an01924a.

[20] C. Wang, F. Madiyar, C. Yu, J. Li, Detection of extremely low concentration waterborne pathogen using a multiplexing self-referencing SERS microfluidic biosensor, J. Biol. Eng. 11 (2017) 1–11, https://doi.org/10.1186/s13036-017-0051-x.

[21] M. Naji, A. Khetani, N. Lagali, R. Munger, H. Anis, A novel method of using hollow-core photonic crystal fiber as a Raman biosensor, Proc. SPIE 6865 (2008), https://doi.org/10.1117/12.763158 68650E-1-68650E–8.

[22] X. Yang, C. Gu, F. Qian, Y. Li, J.Z. Zhang, Highly sensitive detection of proteins and bacteria in aqueous solution using surface-enhanced Raman scattering and optical fibers, Anal. Chem. 83 (2011) 5888–5894, https://doi.org/10.1021/ac200707t.

[23] A. Khetani, J. Riordon, V. Tiwari, A. Momenpour, M. Godin, H. Anis, Hollow core photonic crystal fiber as a reusable Raman biosensor, Opt. Express 21 (2013) 367–370, https://doi.org/10.1364/OE.21.012340.

[24] C.M. Maclaughlin, N. Mullaithilaga, G. Yang, S.Y. Ip, C. Wang, G.C. Walker, Surface-enhanced Raman scattering dye-labeled Au nanoparticles for triplexed detection of leukemia and lymphoma cells and SERS flow cytometry, Langmuir 29 (2013) 1908–1919, https://doi.org/10.1021/la303931c.

[25] G. Perozziello, P. Candeloro, A. De Grazia, F. Esposito, M. Allione, M.L. Coluccio, R. Tallerico, I. Valpapuram, L. Tirinato, G. Das, A. Giugni, B. Torre, P. Veltri, U. Kruhne, G. Della Valle, E. Di Fabrizio, Microfluidic device for continuous single cells analysis via Raman spectroscopy enhanced by integrated plasmonic nanodimers, Opt. Express 24 (2016) 180–190, https://doi.org/10.1364/OE.24.00A180.

[26] C. Catala, B. Mir-simon, X. Feng, C. Cardozo, N. Pazos-perez, E. Pazos, S. Gómez-de Pedro, L. Guerrini, A. Soriano, J. Vila, F. Marco, E. Garcia-rico, R.A. Alvarez-puebla, Online SERS quantification of Staphylococcus aureus and the application to diagnostics in human fluids, Adv. Mater. Technol. 1 (2016), https://doi.org/10.1002/admt.201600163.

[27] A.E. Kandjani, M.J. Griffin, R. Ramanathan, S.J. Ippolito, S.K. Bhargava, V. Bansal, A new paradigm for signal processing of Raman spectra using a smoothing free algorithm: coupling continuous wavelet transform with signal removal method, J. Raman Spectrosc. 44 (2013) 608–621, https://doi.org/10.1002/jrs.4232.

[28] R. Hunter, H. Anis, Genetic support vector machines as powerful tools for the analysis of biomedical Raman spectra, J. Raman Spectrosc. 49 (2018) 1435–1444, https://doi.org/10.1002/jrs.5410.

[29] D.K. Duvenaud, Automatic Model Construction with Gaussian Processes, (2014).

[30] R. Weissleder, A clearer vision for in vivo imaging, Nat. Biotechnol. 19 (2001) 316–317, https://doi.org/10.1038/86684.

[31] E.I. Alarcon, K. Udekwu, M. Skog, N.L. Pacioni, K.G. Stamplecoskie, M. González-Béjar, N. Polisetti, A. Wickham, A. Richter-Dahlfors, M. Griffith, J.C. Scaiano, The biocompatibility and antibacterial properties of collagen-stabilized, photochemically prepared silver nanoparticles, Biomaterials 33 (2012) 4947–4956, https://doi.org/10.1016/j.biomaterials.2012.03.033.

[32] A. Khetani, A. Momenpour, E.I. Alarcon, H. Anis, Hollow core photonic crystal fiber for monitoring leukemia cells using surface enhanced Raman scattering (SERS), Opt. Express 23 (2015) 4599–4609, https://doi.org/10.1364/OE.23.04599.

[33] D.R. Osmon, E.F. Berbari, A.R. Berendt, D. Lew, W. Zimmerli, J.M. Steckelberg, N. Rao, A. Hanssen, W.R. Wilson, Diagnosis and management of prosthetic joint infection: clinical practice guidelines by the infectious diseases Society of America, Clin. Infect. Dis. 56 (2013) 1–25, https://doi.org/10.1093/cid/cis803.

[34] K. Kelley, A. Cosman, P. Belgrader, B. Chapman, D.C. Sullivan, Detection of methicillin-resistant Staphylococcus aureus by a duplex droplet digital PCR assay, J. Clin. Microbiol. 51 (2013) 2033–2039, https://doi.org/10.1128/JCM.00196-13.

[35] P.P. Banada, S. Chakravorty, D. Shah, M. Burday, F.M. Mazzella, D. Alland, Highly sensitive detection of Staphylococcus aureus directly from patient blood, PLoS One 7 (2012), https://doi.org/10.1371/journal.pone.0031126.

[36] O. Opota, A. Croxatto, G. Prod'hom, G. Greub, Blood culture-based diagnosis of bacteraemia: state of the art, Clin. Microbiol. Infect. 21 (2015) 313–322, https://doi.org/10.1016/j.cmi.2015.01.003.



**Robert Hunter** got his start in biosensor research in electrochemical sensors for the agricultural industry during his Bachelor's at the University of Guelph. He joined The University of Ottawa in 2016 as a master's student before fast-tracking to a PhD degree. His current research is focused on the development of biomedical sensors using Raman spectroscopy. Robert is a proponent of multidisciplinary engineering design, and thus integrates microfluidics, data science, photonics, and nanotechnology into his research.

**Ali Najafi Sohi** received his Bachelor's in Mechanical Engineering and his Master's in computational nanomechanics, both from the Sharif University of Technology. He earned his PhD in Mechanical and Mechatronics Engineering from the University of Waterloo in 2013, with a research focus on MEMS sensors and microfabrication. From 2013 to 2015, he was a postdoctoral fellow at the University of Waterloo investigating microcantilever resonators as well as photonic electrochemical sensors. Since 2015, he has been a postdoctoral fellow at the Centre for Interdisciplinary Nanophysics, University of Ottawa, working on single-molecule biosensors and microfluidics.

**Zohra Khatoon** is currently a Research assistant at the University of Ottawa Heart Institute. She received her bachelor's degree in Biomedical Engineering from Uttar Pradesh Technical University in India and a master's degree in Biomedical Engineering at University of Ottawa. Her current work involves preparation and optimization of nanocomposite materials to coat on implants for preventing and treating infections. Her interests mainly lie in implants, artificial organs, nanomaterials, biomaterials and tissue engineering.

**Vincent R. Berthiaume** completed his Bachelor's of Applied Science in Chemical Engineering at the University of Ottawa. As an undergraduate, he held numerous research and industrial internship positions in a variety of fields, including nanotechnology, photonics, heterogeneous catalysis, and plastics manufacturing. Vincent is currently working on an interdisciplinary project relating to the scaled-up synthesis of novel and environmentally-friendly sunscreen and cosmetics ingredients.

**Emilio I. Alarcon** received his B.Sc. in Chemistry at Universidad de Santiago de Chile and moved to Pontificia Universidad Catolica de Chile to pursue graduate studies (MSc/pH.D., 2009). The same year Dr. Alarcon moved to Ottawa with his family for a postdoctoral position at the University of Ottawa. In 2014 University of Ottawa Heart Institute recruited him as an Assistant Professor and Laboratory Director. He has published over 70 articles in peer-reviewed journals, several book chapters and edited 2 books on nanomaterials for biomedical applications. Dr. Alarcon's group works in the development of functional materials and technologies for medical uses (www.beatsresearch.com).

**Michel Godin** received his PhD in physics from McGill University (2004) before becoming a postdoctoral fellow in biological engineering at MIT. He joined the University of

Ottawa in 2008, and is currently an associate professor in the Department of Physics, with parallel appointments in Mechanical Engineering and Biomedical Engineering. He leads a research programme that focuses on using micro- and nano-scale fluid mechanics in single-molecule biosensing applications and for processing therapeutic cells in regenerative medicine applications.

**Hanan Anis** is a professor in Electrical and Computer Engineering at the University of Ottawa. Prior to Joining the University in 2004, Hanan was the co-founder and Chief Technology Officer at Ceyba, an optical long-haul networking company. Hanan also worked at Nortel Networks in different positions conducting pioneering research in various areas of photonics, ranging from device physics to optical networking. She holds a B.Sc from Ain-Shams University (1987), a M.A.Sc (1991) and a Ph.D (1996) from University of Toronto both in Electrical and Computer Engineering. She has numerous journal and conference publications and patents.